

Fixed-Wing Micro Air Vehicles with Hovering Capabilities

Boris Bataillé, Damien Poinot, Chinnapat Thipyopas and Jean-Marc Moschetta

SUPAERO & ONERA
10, Avenue Edouard Belin
31055 TOULOUSE
FRANCE

Boris.bataille@supaero.fr / Damien.poinot@cert.fr /
Thipyopas@supaero.fr / Jean-Marc.Moschetta@supaero.fr

URBAN SURVEILLANCE USING A FIXED WING MAV

Fixed-wing micro air vehicles (MAV) are very attractive for outdoor surveillance missions since they generally offer better payload and endurance capabilities than rotorcraft or flapping-wing vehicles of equal size. They are generally less challenging to control than helicopter in outdoor environment. However, high wing loading associated with stringent dimension constraints requires high cruise speeds for fixed-wing MAVs and it has been difficult so far to achieve good performances at low-speed flight using fixed-wing configurations. The present paper investigates the possibility to improve the aerodynamic performance of classical fixed-wing MAV concepts so that high cruise speed is maintained for covertness and stable hover flight is achieved to allow building intrusion and indoor surveillance.

Monoplane wing plan forms are compared with biplane concepts using low-speed wind tunnel measurements and numerical calculations including viscous effects. Wind-tunnel measurements including the influence of counter-rotating propellers indicate that a biplane-twin propeller MAV configuration can drastically increase low-speed and high-speed aerodynamic performances over the classical monoplane fixed-wing concept. Control in hover flight can highly benefit from the effect of counter-rotating propellers as demonstrated by flight tests.

After describing the flight dynamics model including the prop wash effect over control surfaces, a control strategy is presented to achieve autonomous transition between forward flight and hover flight. Both hardware and software architectures necessary to perform real flight are presented.

1.0 FIXED WING MAV DESIGN

The most common scenario for MAV mission today is urban surveillance. While flying over buildings is already achieved by commercial mini-UAVs, MAV specificity is to be able to fly both outside and inside buildings. Flying outdoor requires the ability to fly fast in order to fulfil the mission in windy condition (wind speed up to 10 m/s, wind gust up to 15 m/s). One common way to achieve this is to use a high wing loading and a powerful propulsion unit with a small diameter, high-pitch propeller. High wing loading is also convenient to counter wind gust disturbance. Flying indoor implies the ability to hover with almost no aerodynamic speed. Although rotating wing systems seems to be the most suitable vehicle for that mission, fixed-wing MAV could prove to be very attractive as well. It is now common in the RC model community to

Bataillé, B.; Poinot, D.; Thipyopas, C.; Moschetta, J.-M. (2007) Fixed-Wing Micro Air Vehicles with Hovering Capabilities. In *Platform Innovations and System Integration for Unmanned Air, Land and Sea Vehicles (AVT-SCI Joint Symposium)* (pp. 38-1 – 38-16). Meeting Proceedings RTO-MP-AVT-146, Paper 38. Neuilly-sur-Seine, France: RTO. Available from: <http://www.rto.nato.int/abstracts.asp>.

Report Documentation Page				Form Approved OMB No. 0704-0188	
Public reporting burden for the collection of information is estimated to average 1 hour per response, including the time for reviewing instructions, searching existing data sources, gathering and maintaining the data needed, and completing and reviewing the collection of information. Send comments regarding this burden estimate or any other aspect of this collection of information, including suggestions for reducing this burden, to Washington Headquarters Services, Directorate for Information Operations and Reports, 1215 Jefferson Davis Highway, Suite 1204, Arlington VA 22202-4302. Respondents should be aware that notwithstanding any other provision of law, no person shall be subject to a penalty for failing to comply with a collection of information if it does not display a currently valid OMB control number.					
1. REPORT DATE 01 NOV 2007		2. REPORT TYPE N/A		3. DATES COVERED -	
4. TITLE AND SUBTITLE Fixed-Wing Micro Air Vehicles with Hovering Capabilities				5a. CONTRACT NUMBER	
				5b. GRANT NUMBER	
				5c. PROGRAM ELEMENT NUMBER	
6. AUTHOR(S)				5d. PROJECT NUMBER	
				5e. TASK NUMBER	
				5f. WORK UNIT NUMBER	
7. PERFORMING ORGANIZATION NAME(S) AND ADDRESS(ES) SUPAERO & ONERA 10, Avenue Edouard Belin 31055 TOULOUSE FRANC				8. PERFORMING ORGANIZATION REPORT NUMBER	
9. SPONSORING/MONITORING AGENCY NAME(S) AND ADDRESS(ES)				10. SPONSOR/MONITOR'S ACRONYM(S)	
				11. SPONSOR/MONITOR'S REPORT NUMBER(S)	
12. DISTRIBUTION/AVAILABILITY STATEMENT Approved for public release, distribution unlimited					
13. SUPPLEMENTARY NOTES See also ADM202416., The original document contains color images.					
14. ABSTRACT					
15. SUBJECT TERMS					
16. SECURITY CLASSIFICATION OF:			17. LIMITATION OF ABSTRACT UU	18. NUMBER OF PAGES 16	19a. NAME OF RESPONSIBLE PERSON
a. REPORT unclassified	b. ABSTRACT unclassified	c. THIS PAGE unclassified			

Fixed-Wing Micro Air Vehicles with Hovering Capabilities

perform hover flight with foam aircraft smaller than 1 meter in wingspan. However that kind of aircraft have a very low wing loading and use large propeller with low pitch to obtain significant static thrust. They are therefore unable to perform forward flight in strong wind conditions nor able to carry the necessary hardware to achieve autonomous flight and the payload. Off the shelf small RC aircraft able to fly both outdoor and indoor does not already exist. Some ideas to conceive such an aircraft will be presented in this chapter.

1.1 Monoplane Wing optimisation

1.1.1 Planform influence

An easy way to maximize lift of the monoplane wing under a maximum dimension L_{\max} constraint would be to maximize its surface adopting a disc plan form of diameter L_{\max} . Although maximum lift is an important parameter for low speed flight, other aspects need to be studied such as lift to drag ratio. Hence, a thorough experimental study has been performed in SUPAERO low speed wind tunnel to determine the best wing plan form in order to maximize lift while maintaining a good lift-to-drag ratio [1]. The different planforms presented in figure 1 were compared using a fixed wing span of 0,2m and a cruise condition of 10m.s^{-1} for 80g mass. Although each planform has its own surface, the 0.2m diameter disc was used as a reference to determine undimensioned coefficients.













Plan form	λ	K	$(L/D)_{\max}$	$C_{L\max}/C_{L\text{cruise}}$	
Zim	1.14	0.54	4.04	3.05	
Zim 2	2.32	0.33	5.11	1.43	
InvZim	1.14	0.58	3.97	2.40	
InvZim 2	2.32	0.35	4.76	1.46	
Plaster	1.40	0.36	4.98	2.21	
Plaster 2	1.80	0.29	5.47	1.88	
Drenalyn	1.26	0.42	4.72	3.07	
Drenalyn 2	2.32	0.30	4.81	1.43	
Trapezoidal	1.00	0.51	4.24	2.79	
Swept 25	2.50	0.35	5.19	1.27	
Circle	1.27	0.38	3.02	2.61	
Square	1.00	0.59	2.95	1.38	

Figure 1: aerodynamic performance (left) and planform description (right)

Maximum lift to drag ratio is shown as well as maximum lift to cruise lift ratio. This last parameter represents the ability to fly at low speed. It clearly appears that the disc planform has low aerodynamic performances in cruise condition and does not provide the best low speed capacity. Plaster and Zimmerman planforms seem to be the best performers at low speed while keeping a good lift-to-drag ratio in cruise conditions.

1.1.2 Aspect Ratio influence

Classical lifting line theory predicts that aspect ratio is the main parameter affecting lift-to-drag ratio. However the Reynolds number and the aspect ratios of MAVs are too low to apply with confidence the lifting line theory results. Therefore, there is a real need for experimental or numerical results. Yet, we can predict that a higher aspect ratio will lead to a higher lift-to-drag ratio but will decrease the maximum lift coefficient. Experimental testing on elliptical plan forms of different aspect ratio confirmed this rule (see figure 2) [1].

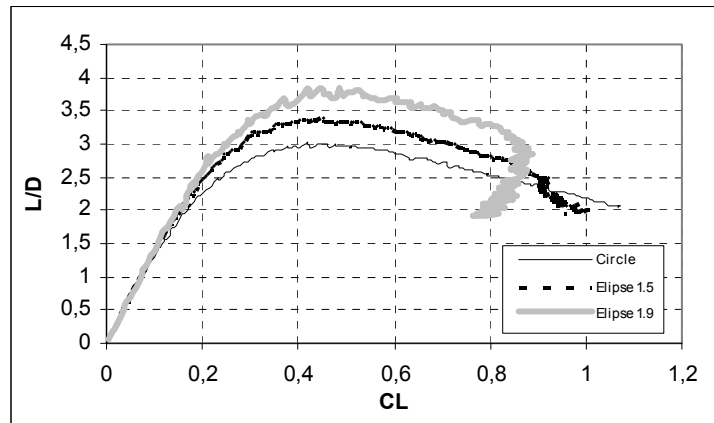


Figure 2: Aspect ratio influence on Lift to Drag Ratio

A thumb rule to ensure a safety margin in cruise condition is to keep a maximum lift coefficient at least twice as large as the cruise lift coefficient. This rule will lead to limit the aspect ratio to a maximum value of approximately 1.7. This can be derived from figure 1.

1.1.3 Camber influence

The wing camber also has a great influence on some aerodynamic properties of the wing. An experimental study has been done in the low speed wind tunnel of SUPAERO. A same planform close to plaster 2 was tested with three different cambers: flat plate, NACA 4400, NACA 8400. The wing span is 0,2m and the wind speed is 10m.s^{-1} . The main aerodynamic characteristics are summed up in table 1.

Camber	$\alpha_0(\text{deg})$	C_{D0}	K	$C_{L\alpha}$	$(L/D)_{\max}$	$C_{L\max}$
Flat Plate	0	0.016	0.30	3.1	8	0.8
NACA 4400	-2	0.025	0.28	3.1	12	1
NACA 8400	-4	0.066	0.18	3.6	7	1.4

Table 1: Effect of airfoil camber on aerodynamic characteristics

As expected, camber produces a shift in the zero lift angle, increases the minimum drag coefficient and improves the maximum lift coefficient. It is interesting to notice that high camber decreases the induced drag coefficient but also leads to a drop in maximum lift-to-drag ratio. Hence, high camber value should be used only for low speed and highly loaded MAV. Moderate camber around 4% would be a good compromise to achieve low speed flight while keeping good aerodynamic performances in cruise condition.

1.1.4 Conclusion

This study on monoplane wing has lead to three important design rules in order to reach low speed flight while keeping good aerodynamics performance in cruise:

- Plan form is of great importance; Zimmerman and Plaster are the best candidates.
- Aspect ratio should be kept under 1.7 to perform low speed flight.
- A maximum lift-to-drag ratio is reached for a moderate camber value.

Fixed-Wing Micro Air Vehicles with Hovering Capabilities

1.2 Biplane Wing configuration

1.2.1 Concept justification

Monoplane MAVs are often designed with a low aspect ratio to maximize the wing area. This leads to a high induced drag especially at high angle of attacks. Previous monoplane MAVs designed at SUPAERO were tested in wind tunnel. Induced drag could represent up to 80% of the total drag. This statement leads to think that a biplane configuration could reduce the induced drag. However, the parasite drag would increase in the mean time. This logic is illustrated in table 2 in which every wing perform at the same lift, speed and overall dimension).

AR	Concept	L _{max} (g.)	Cruise (at 10 m/s, weight 80 g.)					
			L (g.)	D _t (g.)	D ₀ (g.)	D _i (g.)	L/D	D _i /D _t
1	Monoplane	148.5	80.0	13.5	1.9	11.6	5.93	85.9 %
2	Monoplane	96.0	80.0	10.1	1.7	8.4	7.89	83.1 %
2	Biplane	158.3	80.0	8.7	3.4	5.3	9.13	60.8 %

Table 2: Numerical application illustrating the biplane pertinence

It is interesting to notice that the maximum lift L_{max} shown in Table 2 is an experimental value which shows that biplane could perform at least as well as monoplane in term of maximum lift. A theoretical analysis has been done to determine in which conditions the biplane configuration would perform better than a monoplane for a common weight and overall dimension. This resulted in an inequality [1] to satisfy:

$$\frac{V^7 b^7}{W^4} < 690$$

Where b is the wingspan, V is the aerodynamic speed and W the weight of the MAV. This inequality means that the biplane configuration is of interest for low speed, small size and heavy MAVs. For instance, the last prototype developed at SUPAERO is a 30cm wingspan biplane weighting 230g and designed to cruise at 11m.s⁻¹. The ratio equals 164, which justifies the biplane configuration.

1.2.2 Biplane optimisation

The combination of two wings can be done in many ways. A lot of development has already been done in biplane design at a larger scale. However, applying the biplane configuration at low Reynolds needs some further studies. Large quantities of tests were done in wind tunnel to determine the effect of combinations on aerodynamic performances. Four main parameters significantly affect these performances:

- Vertical gap between upper and lower wings.
- Stagger, counted positive when upper wing stands in front of the lower.
- Longitudinal angle between the upper and lower wings.
- Surface ratio.

The result analysis is presented in details in precedent papers [1]. However, the important results are:

- Virtually: the largest gap, the better. Yet, because of maximum dimension constraints and additional parasite drag due to vertical struts, the gap will be limited. Gap increase leads to less interaction

between the two wings which results in a higher lift to drag ratio, a larger maximum lift and a smaller induced drag.

- Positive stagger creates a higher maximum lift. Negative stagger performs poorly at high angle of attack because the fore wing stall triggers the aft wing stall.
- Longitudinal angle has a large effect on stall angle, parasite drag, lift to drag ratio and maximum lift. Small negative angle decreases parasite drag and increases the maximum lift.
- Total drag varies with the wings surface ratio. It reaches a minimum for a ratio of 1 but is almost constant until the surface ratio drops under 0.6.

1.2.3 Propeller influence

The ratio between propeller diameter and wingspan of a MAV can be close to 1 which is very different from other UAVs. Hence, propwash effects are essential to the aerodynamic performances. Several wind tunnel tests were made to compare different configurations as it is shown on figure 3 [2].

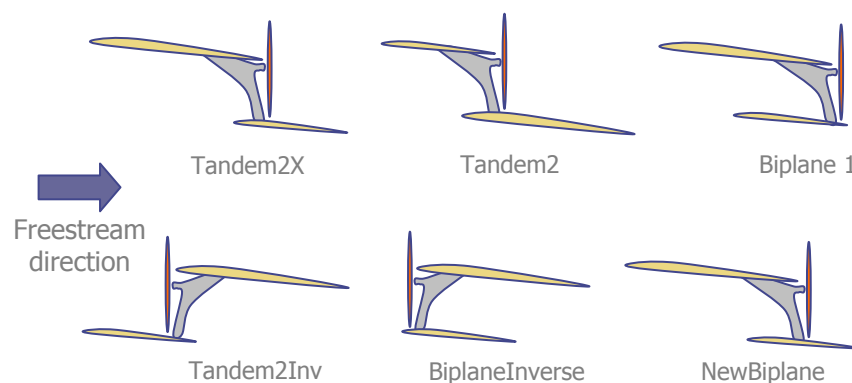


Figure 3: different wing and propeller configurations

Table 3 presents the results of the different configurations. For each speed, the results are given for a longitudinal equilibrium condition ($Lift=Weight$ and $Thrust=Drag$). It has been found that the positive stagger biplane equipped with two counter rotating propellers positioned at the trailing edge of the fore wing was the most effective configuration to achieve low speed flight. Stall is delayed and both upper and lower wing get a lift increase while the induced drag do not increase drastically. Moreover the lower wing sees a high effective angle of attack in the pusher configuration whereas it sees a reduced angle of attack in the tractor configuration. The aerodynamic effects responsible of this behaviour are illustrated on figure 4.

Fixed-Wing Micro Air Vehicles with Hovering Capabilities

Model	Velocity 5 m/s			Velocity 10 m/s		
	I (Amp)	C_L (max)	$\frac{L_{max}}{W}$	I (Amp)	C_L (max)	$\frac{L_{max}}{W}$
Tandem2	1.05	2.0	1.19	1.4	1.2	2.86
Tandem2x	1.4	1.9	1.13	1.4	1.3	3.09
Tandem2 Inv.	>1.5	1.4	0.83	1.05	1.0	2.38
Biplane	1	1.8	1.07	1.05	1.2	2.86
BiplaneInverse	>1.5	1.6	0.95	1.05	0.9	2.14
NewBiplane	1.05	2.1	1.25	1.05	1.35	3.21

Table 3: powered configurations results

Numerical simulation has been applied to this configuration to obtain a better knowledge of the local interaction between propellers and wings. Numerical results confirmed the experimental conclusion. Propeller turning in the opposite direction of wing tip vortex improves slightly the induced drag of the MAV and also has an advantage for flight dynamics. Indeed, a differential thrust will create a roll torque in the same direction as the yaw torque.

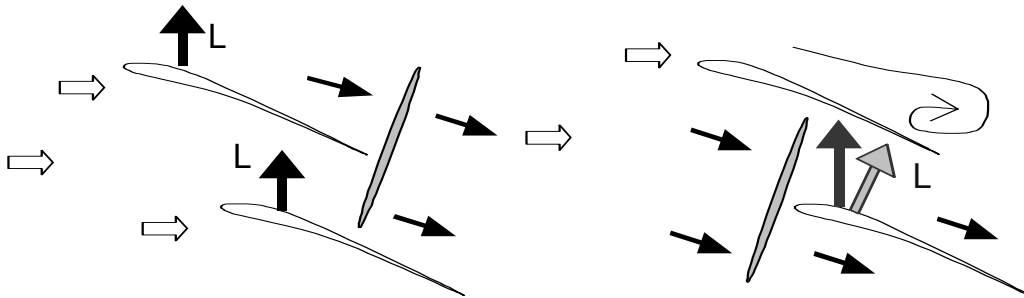


Figure 4: Tractor versus Pusher configuration

1.3 The TYTO prototype

1.3.1 Design and wind tunnel tests

A prototype inheriting from the design expertise developed at SUPAERO has been produced. The TYTO configuration is derived from the NewBiplane (see figure 3). Lower wing has been modified so that it is linked to the upper wing tips. A horizontal tail has been added for static balance as well as dynamic control. A larger wind tunnel model was tested in a large elliptic wind tunnel at high speeds (10 to 20m.s^{-1}). A smaller wind tunnel model was then built to study the aerodynamic performances at very low speeds (5m.s^{-1}) and to improve the upper wing performances.

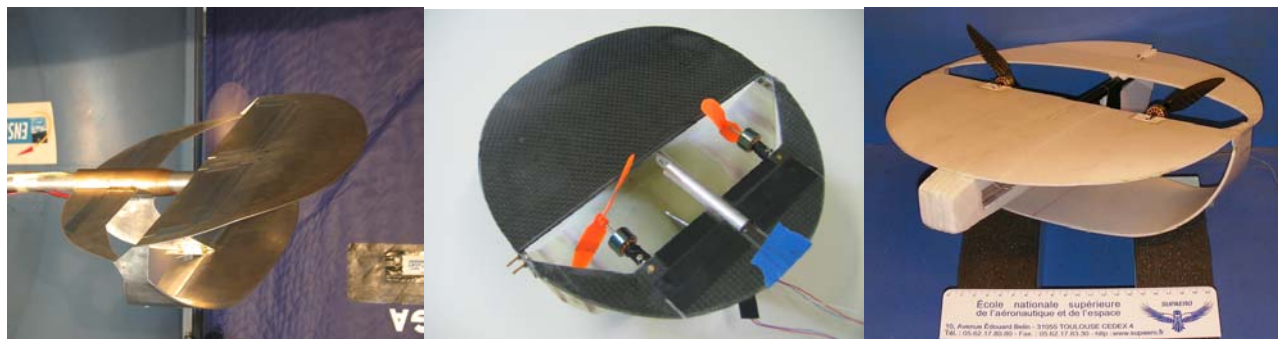


Figure 5: TYTO wind tunnel models and first prototype

The wind tunnel measurements lead to equip the TYTO with only one pair of elevons on the horizontal tail as it proved to be efficient enough for control at every speed. This good efficiency is mainly due to the fact that the elevons are located in the propellers stream.

1.3.2 Prototype and test flights

The TYTO prototype has a 30cm wingspan and a 230g mass. Its optimal cruise speed is 11m.s^{-1} . It carries a 30g payload located in front of the upper wing. This payload consists in a colour CCD camera with 2 axis control. The propulsion unit is able to deliver a 320g static thrust which ensures the theoretical capacity to perform hover flight. It is composed of two brushless electric motor mounted with carbon propeller (5" diameter). The mass proportion of the different subsystems is presented in figure 6.

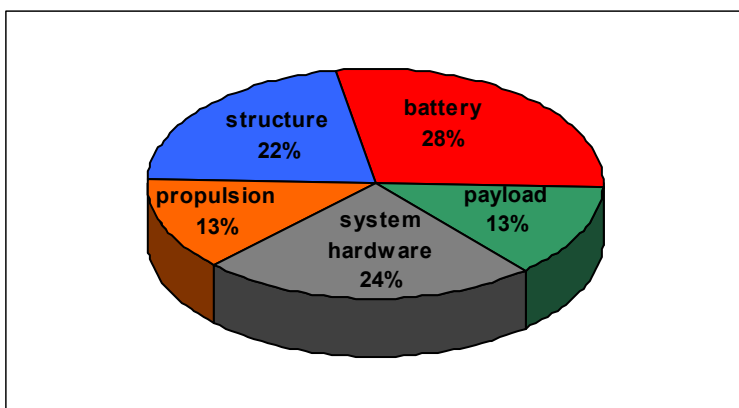


Figure 6: TYTO subsystems mass proportion

Several successful test flights took place in February. Flight speeds from 5m.s^{-1} up to 18m.s^{-1} were reached. Hover flight could not be performed because of torque issues. This should be fixed by the use of new counter rotating propellers. First autonomous flights are planned for the end of spring. TYTO aims at competing in MAV07 event. Its current auto pilot architecture will permit outdoor flight on a large speed envelope but will not control hover flight.

Fixed-Wing Micro Air Vehicles with Hovering Capabilities

1.4 The VERTIGO prototype

A parallel development was lead on a bigger and non optimized platform called VERTIGO. This project aims at demonstrating autonomous transition between forward and hover flight. The size and geometrical configuration were chosen so that system integration and control laws will be easier to realise. The aircraft consists in a main flying wing equipped with large elevons crossed by a symmetrical rudder. A counter rotating axial rotor is mounted at the front of the wing. Its wingspan is 70cm and its mass is about 1.5kg. An experimental campaign is being led to determine the efficiency of elevons in hover flight.



Figure 7: VERTIGO early prototype

Both TYTO and VERTIGO can be gathered in the same category of VTOL: the tilt body. Indeed hover flight is reached by tilting the whole aircraft to vertical. Experience gathered on the VERTIGO concept will be used to achieve autonomous vertical flight with the TYTO.

2.0 AUTONOMOUS TRANSITION FROM FORWARD FLIGHT TO HOVER FLIGHT FOR A MICRO AIR VEHICLE (MAV)

A MAV is a flying vehicle equipped with an onboard control system which grants it full autonomy by operation guidance, navigation and control tasks. The process involves three steps: guidance equipment and software first compute the aircraft trajectory required to satisfy the mission objectives, navigation then tracks the vehicle's current position and attitude, and flight control then transports the aircraft along the required flight path in order to accomplish the mission. Functions of the control system also include communication with the operator and the ground control station before, during and after flight.

The automatic control of a UAV can be made only if we approach all the aspects. That is why, in introduction, we speak about the UAV system. It is what we describe the automation work of UAV system by means of figure 8. This figure explains the interaction between 4 entities: "the Micro Air Vehicle", "the Embedded System", "the Development tools" and "the ground station".

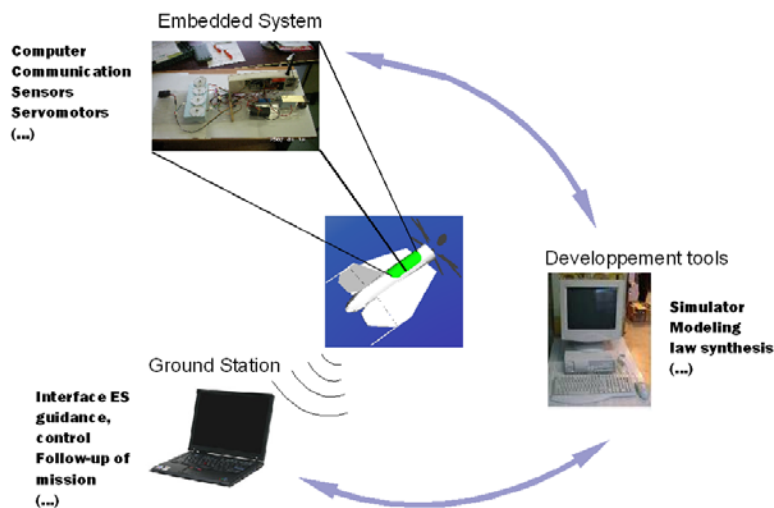


Figure 8: UAV system

We speak in this part of the autonomous control for fixed wing Micro Air Vehicle capable of fast forward flight and hovering flight (we can see the principle of this mechanism in figure 9). It supposes that the aircraft tilts completely on its pitch axis during the transition and that the propeller stream is efficient enough for the control at low speed (The control being achieved by deflection of airflow);

We develop our presentation in 3 parts: in the first part we will treat the aerodynamic modelling (especially how the propeller stream is modelled), the simulator specifically created for this application and some simulation results. In the second part we will describe the operating mode of the autopilot. Finally in the third part we shall briefly describe the embedded system capable of handling automatic transitions between flight phases.

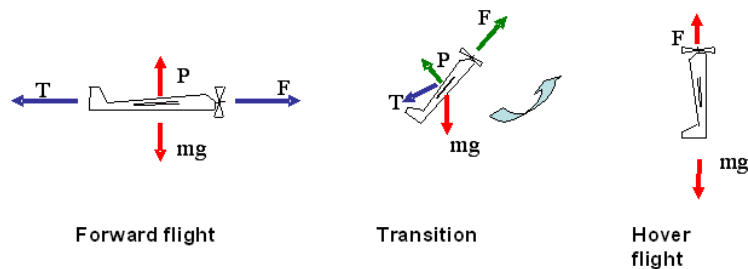


figure 9: transition principle

2.1 Modelling

The behaviour of a machine with fixed wing in forward flight is well known. However, its behaviour in transition phase has to be modelled carefully. First, we will define here the dynamics of flight equations. We will observe that for a correct modelling of the hover flight phase, we have to introduce the speed due to the propeller. Furthermore, a continuous computation of this speed during the transition and in the hover flight

Fixed-Wing Micro Air Vehicles with Hovering Capabilities

phase must be done. These equations are written in quaternion formalism with respect to the aircraft frame. For general equations you can consult [4], and for specific modelling [5].

2.1.1 Dynamics equations

2.1.1.1 Equations of efforts

$$\frac{du}{dt} = \frac{\rho}{2m}(-S_a V_a^2 C_A) + \frac{F_x}{m} - qw + vr + 2g(q_1 q_3 - q_0 q_2)$$

$$\frac{dv}{dt} = \frac{\rho}{2m}(S_a V_a^2 C_Y) + \frac{F_y}{m} + 2g(q_2 q_3 + q_0 q_1) - ru + pw$$

$$\frac{dw}{dt} = \frac{\rho}{2m}(-S_a V_a^2 C_N) + \frac{F_z}{m} + 2g(q_0^2 + q_3^2) - pv + qu$$

2.1.1.2 Equations of moments

$$(AC - E^2) \frac{dp}{dt} = \left[\left(\frac{1}{2} \rho l (S_a V_a^2) \right) [(C_l)C + (C_n)E] + (BC - C^2 - E^2)qr - E(B - A - C)pq \right]$$

$$(B) \frac{dq}{dt} = \left[\left(\frac{1}{2} \rho l (S_a V_a^2 C_m) \right) + (C - A)pr - (p^2 - r^2)E \right]$$

$$(AC - E^2) \frac{dr}{dt} = \left[\left(\frac{1}{2} \rho l (S_a V_a^2) \right) [(C_l)E + (C_n)A] + E(B - A - C)qr + (E^2 - A(B - A))pq \right]$$

2.1.1.3 Propeller stream

The aerodynamic speed is denoted V_a (previous equation). In classical modelling it's only due to the contribution of the object motion in air. Here we expand this modelling and define a new variable: V_h (Following equation). This variable represents airflow due to the propeller motion and changes the aerodynamic behaviour. The principle theory used to establish V_h is momentum theory and an empirical part. (We can see details here [5]).

$$V_a = V_0 \cos(\alpha_{Ra}) + V_H \cos(\alpha_0) \quad \text{With} \quad \alpha_{Ra} = \arctan \frac{V_H \sin(\alpha_0 + \alpha_{Ra})}{V_0 + V_H \cos(\alpha_0 + \alpha_{Ra})}$$

$$V_H = 0.6 \exp \left(-\frac{V_0 \cos(\alpha_0 + \alpha_{Ra})}{2.5} \right) * \left[-V_0 \cos(\alpha_0 + \alpha_{Ra}) + \sqrt{[V_0 \cos(\alpha_0 + \alpha_{Ra})]^2 + \frac{F_x}{\frac{1}{2} \rho S_H}} \right]$$

This modelling results in a system of equations valid in the entire speed range. With this system we can define a strategy of command ensuring the stability.

2.1.2 Simulation

The UAV physical model is entirely simulated in a Matlab/Simulink environment. First of all this model is used to define and set up the different control loops of the autopilot. In a second time it is used for flight software validation using S-functions in the same simulink model. Finally this simulation tool is used for flight test data analysis, which eventually leads to improvements of both the physical model and the autopilot.

In this part we can observe the result of propeller airflow modelling. This simulation result represents the transition from forward to hover flight. We can see the airspeed (in black) decreases from 10 m/s to 0 m/s, and during this time we can observe the increasing of propeller flow velocity according to the equation described in (2.1.1.2).

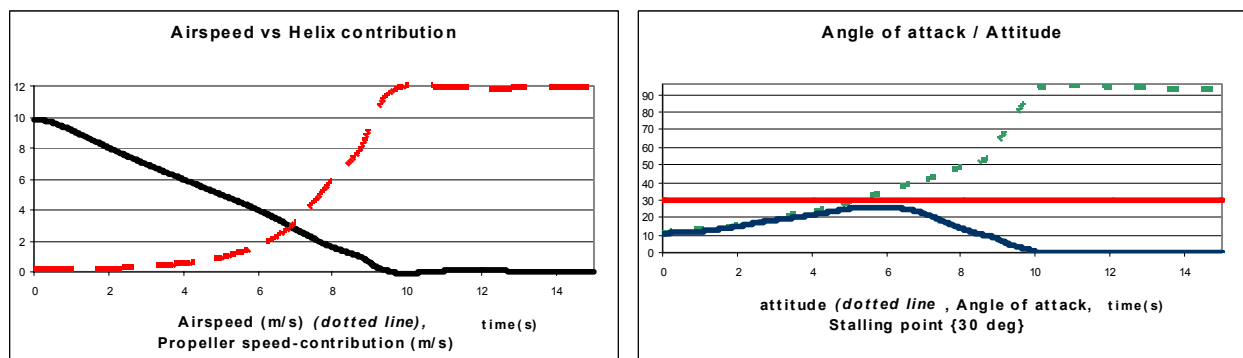


Figure 10: Propeller flow contribution

The second simulation result (figure 10) shows the other interest of modelling the propeller stream. During the transition we observe the angle of attack versus attitude. In forward flight, the equilibrium is reached for an attitude (green plot) of 10 degrees (time 0) and in hover flight the equilibrium is reached for an attitude of 94 degrees (time 14). In the mean time, the angle of attack (blue plot) always remains below 30 degrees. It's a very interesting result because we can say: **The controllability is possible during the transition.**

2.2 Autopilot

2.2.1 Generality

We present in this part the principle of the embedded autopilot system, which ensures flight phase transition: the gain-sequencing (GS) technique. Two main points lead to use the GS technique: first, the dynamic of the system is evolving with the flight conditions. Finally, the real time embedded system requires a simple control law which calculates very quickly the command for actuators.

Fixed-Wing Micro Air Vehicles with Hovering Capabilities

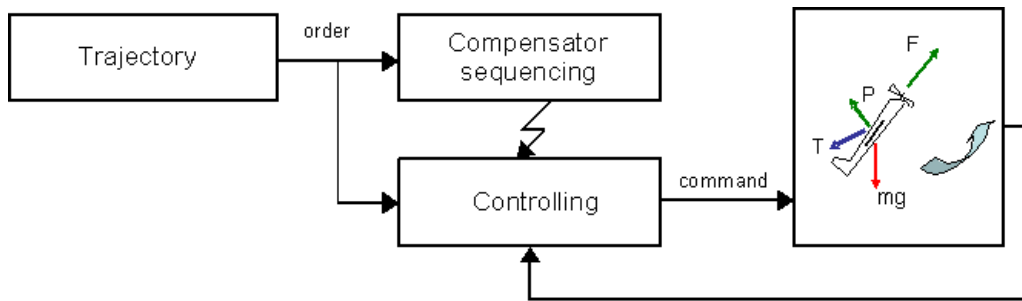


Figure 11: Autopilot Structure

The structure of the autopilot is presented in three blocks. First, “Trajectory” is the strategy chosen to achieve the transition between flight phases. For instance: The body is tilted with linear decreasing of airspeed, (from 10 m/s to 0 m/s) according to keep a constant altitude. The control order comes out from the trajectory block, and is dispatched into two blocks: “Compensator Sequencing” and “controlling”. The controlling block contains all control gains that stabilize the MAV and the Compensator Sequencing block chooses the good control gains by an interpolation technique in function of trajectory strategy. The gains are sequenced. If the order changes then the control gain is changed.

2.2.2 Control-gain determination.

We present in this paragraph the method used to determinate the control-gain. It is an iterative method.

- Analytical linearization ($A(x)$, $B(x)$, $C(x)$, $D(x)$) [off line operation]
- Flight envelope cutting (A_i , B_i , C_i , D_i) [off line operation]
- At each point, Control gain Computing (K_i) [off line operation]
- Gain – Sequencing by interpolation [in line operation]

The analytic linearization allows the extraction of the model in particular point in the entire flight envelope. We used the general dynamics equation (quickly presented in modelling paragraph) and the propeller stream contribution. The flight envelope cutting applies numerical value at the analytical linearization (with particular aerodynamic, dynamic and kinematics model). Then we can compute the control gain and ensure the stabilization and control in every flight condition. When this operation is complete, we can work onboard, and apply the good compensator for particular flight point using the gain-sequencing.

2.3 Embedded system

2.3.1 Hardware architecture

In this paragraph we present the components used for an autonomous micro air vehicle (the general architecture is presented in figure 11). In order to achieve the autonomous control and transition from forward flight to hover flight, the following hardware is required:

- Sensors

Inertial Measurement Unit (IMU), all attitude (used quaternion formalism) to be composed of 3 accelerometers, 3 gyrometers and 3 magnetometers. The IMU name is MTx (xsens).

Global Positioning System (GPS), 4 Hz.

These two elements are sufficient for stabilization, control and guidance but if an accurate measure of the ground distance is needed (for automatic landing), a specific sensor should be used (for example ultrasonic sensor, or radar sensor)

- On board calculator

The core of the system architecture is a Motorola MPC555 Central power unit. This is a high speed, 32 bits device which features and floating point unit designed to accelerate the advanced algorithms necessary to support complex application. It is powerful enough to perform calculation (Gain –sequencing in line, for instance) and ensures a 40 Hz control loop with a comfortable safety margin.

2.3.2 Software architecture

The role of the software is to manage, coordinate and control the different subsystems and interfaces. The flight software coded in C++ language is directly implemented on the 4MB flash memory of the CPU chip and is designed on a real time concept. Real-time operation are managed in the synchronous approach, that is to say calculations for different tasks are made as soon as they appear in chronological order without pre-emption, as their execution time is very short. (The schematic architecture is present figure 12). If you want further information you can consult [3]

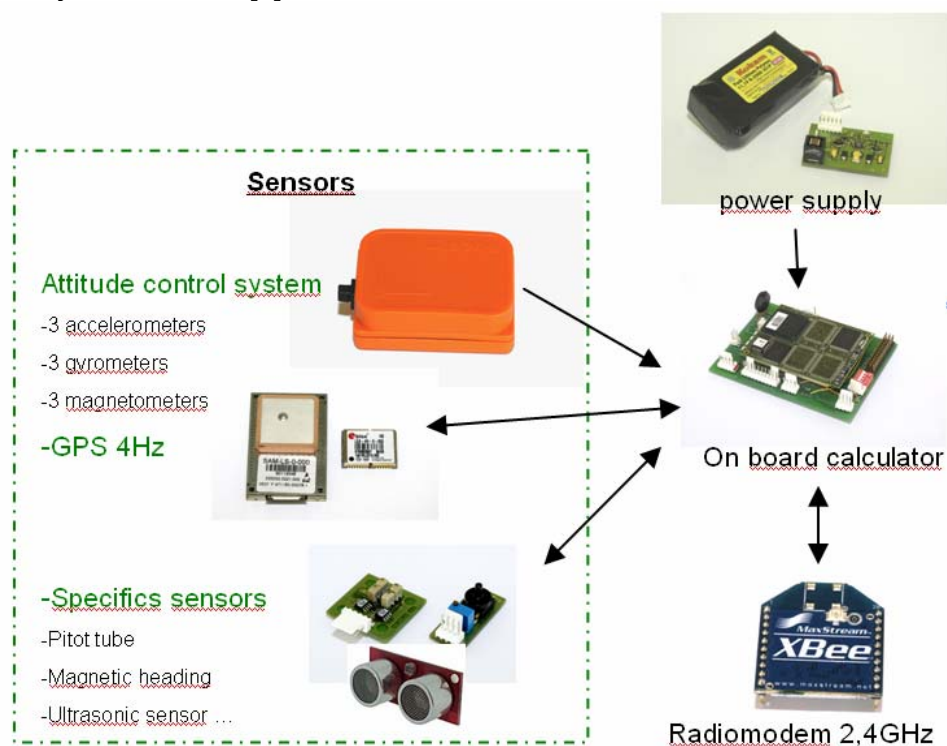


Figure 11: Hardware architecture

Fixed-Wing Micro Air Vehicles with Hovering Capabilities

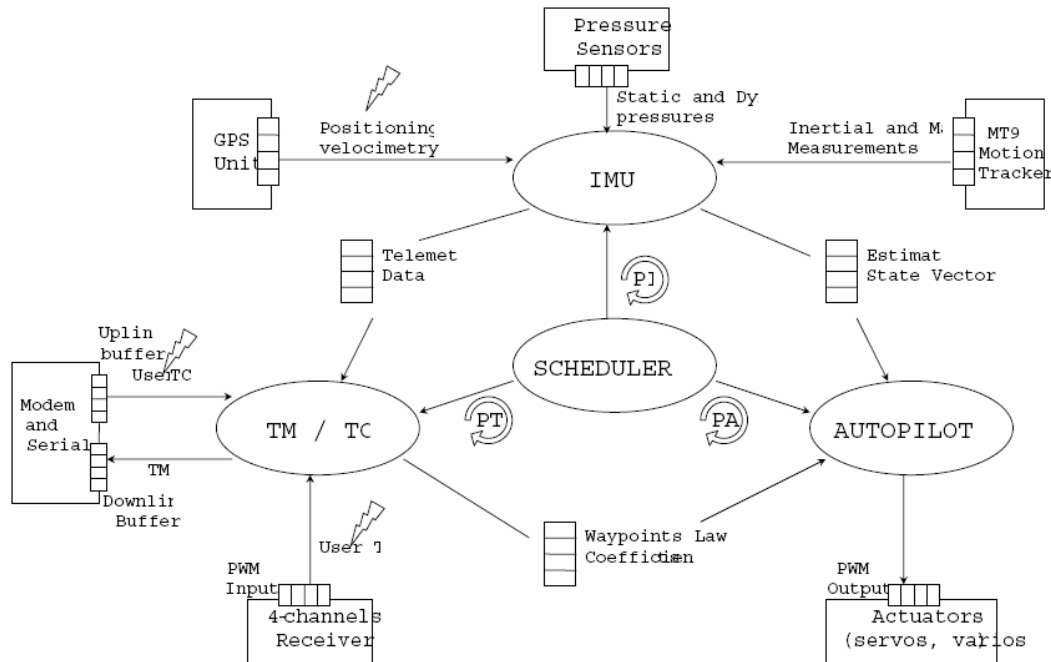


Figure 12: Software architecture

3.0 BIBLIOGRAPHY

- [1] **Aerodynamic Performance of Biplane Micro Air Vehicle.** Accepted for publication in the Journal of Aircraft, 2007. Jean-Marc Moschetta, Chinnapat Thipyopas. *Ecole nationale supérieur de l'Aéronautique et de l'Espace.*
- [2] **A Low-Speed Fixed-Wing Micro Air Vehicle.** EMAV 2006. Chinnapat Thipyopas, Jean-Marc Moschetta. *Ecole nationale supérieur de l'Aéronautique et de l'Espace.*
- [3] **Conception of an UAV Generic Mission System.** ICAS 2006. Damien Poinot, Jacques Lamaison, Alain Hostallier, Caroline Bérard. *Ecole nationale supérieur de l'Aéronautique et de l'Espace.*
- [4] **The Dynamics of Flight – The equations.** Wiley 1998. Jean Luc Boiffier. *ONERA centre de Toulouse Département commande des système et dynamique du vol. & ENSAE.*
- [5] **Contribution au développement du pilote automatique de la Drenalyn.** Projet de Fin d'Etude 2005-2006. Tiago de Castro Grossinho, Damien Poinot, Jacques Lamaison, Caroline Bérard. *Ecole nationale supérieure de l'Aéronautique et de l'Espace.*
- [6] **Fixed wings mav controlled by deflection of airflow in a hover flight phase.** EMAV 06. Braunschweig (Germany). Damien Poinot, Boris Bataillé, Alain Piquereau, Caroline Berard. *ONERA centre de Toulouse & ENSAE.*
- [7] **Analyse du comportement dynamique de drones miniatures à voilure tournante.** F. Marchand et C. Melet. Rapport technique RT 1/10352 DPRS, ONERA, 2005.

[8] **Preliminary Modelling, Control, and Trajectory Design for Miniature Autonomous Tailsitters.** Nathan B. Knoebel, Stephen R. Osborne, Deryl O. Snyder, Timothy W. McLain, Randal W. Beard, Andrew M. Eldredge. *Brigham Young University, Provo, UT 84602.*

[9] **Nonlinear Control Systems Design Project – Tailsitter.** *Randal W. Beard, Wei Ren. Preprint. February 27, 2006.*

Fixed-Wing Micro Air Vehicles with Hovering Capabilities

